Black Sea Journal of Engineering and Science
doi: 10.34248/bsengineering.1373961

Open Access Journal
e-ISSN: 2619 – 8991

Research Article
Volume 7 - Issue 1: 89-95 / January 2024

PI-PD CONTROLLER DESIGN BASED ON WEIGHTED GEOMETRIC CENTER METHOD FOR TIME DELAY ACTIVE SUSPENSION SYSTEMS

Abdullah TURAN[1], Hüseyin AGGUMUS[1], Mahmut DASKIN[2,3]*

[1]*Sirnak University, Department of Mechanical and Metal Technologies, 7300, Sirnak, Türkiye*
[2]*İnönü University, Faculty of Engineering, Department of Mechanical Engineering, 44280, 10 Malatya, Türkiye*
[3]*Cranfield University, Energy and Sustainability Theme, MK43 0AL, Cranfield, United Kingdom*

Abstract: In this study, a PI-PD controller was designed via weighted geometric center method (WGC) for a quarter vehicle model to suppress the vertical vibrations. The proposed design is based on finding the weighted geometric center of the area formed by the control parameters that make the system stable. The WGC method has two main stages. First, an area formed by the parameters of the PD controller (k_f, k_d) in the inner loop is obtained and the weighted geometric center of this area is calculated. Then, using these obtained parameters, the inner loop is reduced to a single block, and the parameters of the PI controller in the external loop (k_p, k_i) are calculated using the stability boundary curve as in the first step, and the weighted geometric center is calculated. The simulation results show that the PI-PD controller designed with the weighted geometric center method offers successful responses for the time delay quarter vehicle system.

Keywords: Quarter vehicle model, PI-PD controller, Weighted geometrical center method, Stability

***Corresponding author:** İnönü University, Faculty of Engineering, Department of Mechanical Engineering, 44280, 10 Malatya, Türkiye
E mail: mahmut.daskin@inonu.edu.tr (M. DASKIN)
Abdullah TURAN https://orcid.org/0000-0002-0174-2490
Hüseyin AGGUMUS https://orcid.org/0000-0002-7158-677X
Mahmut DASKIN https://orcid.org/0000-0001-7777-1821

Received: October 10, 2023
Accepted: December 25, 2023
Published: January 15, 2024

Cite as: Turan A, Aggumus H, Daskin M. 2024. PI-PD controller design based on weighted geometric center method for time delay active suspension systems. BSJ Eng Sci, 7(1): 89-95.

1. Introduction

The aim of the studies on suspension systems, which is one of the most important parts of vehicle dynamics, is to suppress the vibrations that occur in the vehicle due to road defect/roughness and to increase the vehicle's handling. To achieve this, basically three different control applications are used, namely active (Kararsiz et al., 2021) semi-active (Paksoy and Metin, 2019), and passive (Paksoy and Metin, 2020). Although active control applications show high performance, they require high cost. Semi-active control applications have higher performance, and they require less cost compared to passive control applications. Passive control applications exhibit lower performance compared to the other two control applications, while also being more affordable.

Adaptive, classical PID and robust control types, applications of quarter vehicle model on vibration control are available in the literature. Uncertainties in the system model, different operating conditions and high-performance requirements require more efficient control systems such as adaptive ones.

However, the intricate nature of adaptive control design poses challenges, rendering the process arduous. Therefore, researchers tend to use robust control methodologies to avoid poor performance output due to system and modeling uncertainties.

Adaptive and robust controllers either require very complex control and/or adaptive architectures, or the desired performance is achieved with high-order controllers.

In recent years, low-order PID controllers, which are simply used to control higher-order operations, are preferred. PID controller is widely used in industrial applications due to the simplicity of the control structures, easy to understand, easy to maintain and low cost (A Turan et al., 2019) . In addition, many methods such as Ziegler-Nichols step response, Ziegler-Nichols final cycle, Cohen-Coon internal model control, error-integral criterion adjustment formulas, gain and phase margin are available in the literature to determine the optimum parameters (Åström et al., 1993; Åström and Hägglund, 1995; Ho et al., 1995; Ziegler and Nichols, 1942). However, in some cases, the closed-loop responses of the mentioned controllers may not be at the desired level (Åström et al., 1993). In the studies on the development of these methods, the desired answers are not always obtained (Zhuang and Atherton, 1993). Therefore, the studies carried out to determine the optimum controller parameters are still up to date.

The design studies for tuning the PID control parameters can be classified into three categories as optimization (Ho et al., 1998; Pai et al., 2010; A Turan and Aggumus,

2021; Turan, 2021; Yeroglu et al., 2009), tuning formulas for a particular class (Chidambaram and Sree, 2003; Luyben, 2003), and studies for determining the controller parameters region (Atic et al., 2018; Onat, 2013; Ozyetkin et al., 2018). In the literature, stability boundary location method in the calculation of PID parameters seems to have attracted more attention of researchers recently. PID controllers tuned with the proposed methods have performed successfully for certain classes of systems. However, PID controllers have inherent limitations in controlling time-delayed unstable processes (Kaya, 2003; Kaya, 2016).

Compared to traditional PID controllers, PI-PD controller structure has advantages. While PID controllers may not always show the desired performance in the control of unstable and resonant systems, PI-PD controllers show effective performance for the aforementioned systems (Kaya, 2016; Park et al., 1998; Tan, 2009). In addition, the number of PI-PD control parameters is one more than the number of PID control parameters.

Some of the important studies presented in the literature on PI-PD controller design can be found in (Nema and Padhy, 2015; Özbek and Eker, 2016; Ozyetkin et al., 2020; Padhy and Majhi, 2006). However, studies on PI-PD are not sufficient and the parameters of the controllers are adjusted after complex processes.

The proposed method in this study is based on drawing the stability boundary location, which is dependent on the controller and frequency parameters, in the parameter plane. The weighted geometric center method, which was first proposed for the PI control of time-delayed systems, is based on the stable area calculation timeline of the mentioned control parameters (Onat, 2013) .The mentioned WGC method has been used in successful applications in PI/PI-PD/PID design so far (Oant et al., 2021; Onat, 2018; Onat et al., 2017; Onat et al., 2012; Ozyetkin et al., 2018; Ozyetkin et al., 2019; Ozyetkin et al., 2020; Turan et al., 2019). The advantage of the WGC method over other methods (genetic algorithm (Ahmad et al., 2014), LQR (Kumar and Jerome, 2013), Jaya algorithm (Sain et al., 2018), Ziegler-Nichols tuning (Ho et al., 1996), Astrom-Hagglund autotune (Ho et al., 1997)) is that the control parameters are calculated numerically without any optimization process.

This study consists of five sections. In Section 2, the quarter vehicle model is presented. The design procedure of the PI-PD controller is then given in Section 3. The simulation results are presented in Sections 4. The conclusions are drawn in Section 5.

2. Materials and Methods

2.1. Quarter Vehicle Model

The quarter vehicle model, which is widely preferred in studies due to its simple structure, is defined with two degrees of freedom, z_1 and z_2, as seen in Figure 1. In the model, there are two masses named m_1 and m_2, one suspended and the other one unsuspended, respectively (Paksoy and Metin, 2020). The connection between these masses is the suspension system. Suspension spring coefficient is k_1 and suspension damping coefficient is c_1. The spring coefficient of the wheel is k_2 and since the damping value is very small, it has been neglected. h is the path input applied to the model. The equations of motion of the quarter vehicle model seen in Figure 1 are given in equation 1 and 2.

$$m_1\ddot{z}_1 + c_1(\dot{z}_1 - \dot{z}_2) + k_1(z_1 - z_2) + f_u = 0 \quad (1)$$

$$m_2\ddot{z}_2 - k_1(z_1 - z_2) + k_2(z_2 - h) - f_u = 0 \quad (2)$$

The f_u expressed in the equations represents the force produced by the controller. Mass values for vehicle parameters are m_1=338.8 kg, m_2=59 kg. Spring coefficients are k_1=15000 N/m, k_2=15000 N/m. The damping value of the suspension is c_1=600 N.s/m (Paksoy and Metin, 2020) . $G_p(s)$ is the transfer function of the system and it is given in equation 3.

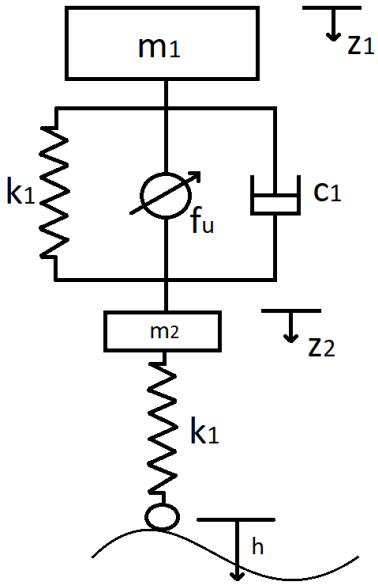

Figure 1. Quarter vehicle model.

$$G_P(s) = \frac{-0.019908s^2 + 1.7927 * 10^{-8}s - 9.5276}{s^4 + 11.9446s^3 + 3518.955s^2 + 5716.5781s + 142914.4519} \quad (3)$$

PI-PD Controller Design Procedure

The diagram of the PI-PD control system is shown in Figure 2. Through the inner loop with the PD controller shown in the figure, the transfer function of the system is reduced and its response is improved. In other words, it can transform the unstable process in the open loop into the stable process in the open loop. Thus, the poles of the obtained system are better positioned. Then, the performance of the system is tried to be increased with the PI controller in the second loop.

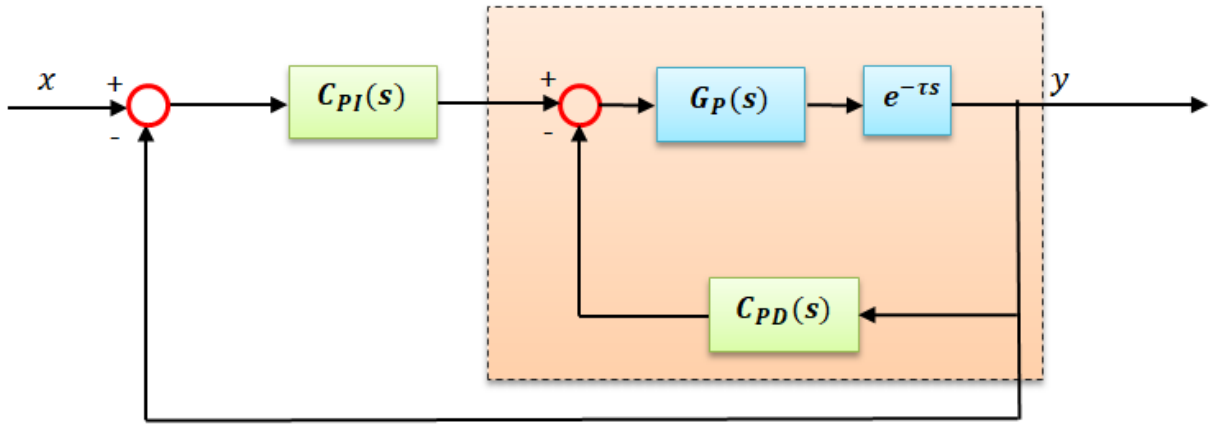

Figure 2. PI-PD Control System with time delay.

The transfer function of the system can be described as in equation 4.

$$G_P(s) = \frac{N_P(s)}{D_P(s)} \quad (4)$$

Here, τ represents delay time of the system. C_{PD} and C_{PI} are models of PD and PI controller, respectively (equations 5 and 6).

$$C_{PD}(s) = \frac{N_{PD}}{D_{PD}} = \frac{(k_f+100k_d)s+100k_f}{s+100} \quad (5)$$

$$C_{PI}(s) = \frac{N_{PI}}{D_{PI}} = \frac{k_p s+k_i}{s} \quad (6)$$

Here, k_d and k_f are the derivative and proportional gains of the PD controller. k_p and k_i symbolize the proportional and integral gains of the PI controller, respectively. The closed loop characteristic equation with PD controller is given in equation 7.

$$\Delta_{PD}(s) = D_P(s)D_{PD}(s) + N_P(s)N_{PD}(s)e^{-\tau s} = 0 \quad (7)$$

The proposed design procedure consists of three steps;

Step1. By calculating the stable area parameters of the C_{PD}, the stability region in the k_d-k_f plane is obtained. For this, if $s = j\omega$ and $e^{-\tau j\omega} = \cos(\tau\omega) - jsin(\tau\omega)$ changes are applied in equation 8.

$$\Delta_{PD}(\tau\omega) = D_P(\tau\omega)D_{PD}(\tau\omega) + N_P(\tau\omega)N_{PD}(\tau\omega)\,(\cos(\tau\omega) - jsin(\tau\omega)) = 0 \quad (8)$$

Here, if Δ_{PD} is separated to its real and imaginary part equation 9 is obtained.

$$\Delta_{PD} = R_{\Delta,PD} + jI_{PD} = 0 \quad (9)$$

Here $R_{\Delta,PD}$ and $J_{I\Delta,PD}$ are functions of k_d, k_f and ω. By equating the real and imaginary parts of Δ_{PD} to zero, two equations with two unknowns with parameters (k_d, k_f) are obtained. The system of equality is given in equation 10.

$$R_{\Delta,PD}(k_f, k_d, \omega) = 0\,, I_{\Delta,PD}(k_f, k_d, \omega) = 0 \quad (10)$$

The equation (linear) system based on frequency (ω) is solved and then a curve is drawn with the k_d-k_f parameters obtained in the k_d-k_f plane. Finally, the stable region of this area and the WGC is determined.

2.2. Calculation of WGC Point

The WGC method is based on two principles. First, it is the computation of the region of stabilizing controller parameters. For this, the stability boundary curve method is used. The second basis of the method is to determine the WGC point of the stability area by means of the parameters forming the boundary curve of the stability region. To understand the WGC method better, the design of the PD controller in the inner loop is detailed. In this context, if two equations with two unknowns (k_d, k_f) in Eq. (7) are solved depending on the frequency (ω) (rad/s), the stability boundary locus and stability region of the PD controller is obtained as in Figure 3. Time delay of the system is considered as 0.1 s.

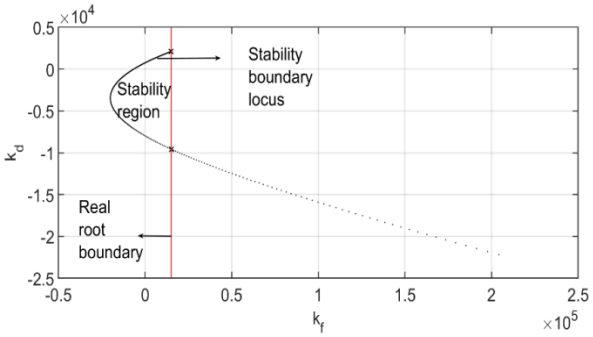

Figure 3. The stability boundary curve and stability region of PD controller.

The real root boundary line, which is formed by the change of system parameters, is the line shows the location of the closed-loop roots in the s-plane. In Figure 3, The stability region is obtained by choosing random points from different areas seen in the graph and using the Hurwitz stability test method.

In the figure, the stability boundary curve is obtained with $\omega \in [0, 15.8]$. The stability boundary curve is represented as pairs (k_f, k_d) corresponding to each value of ω. As can be seen in Figure 2, the points are located at different intervals for each ω value. The line k_f = 15000 indicates the boundary of the stability boundary curve. Closed stability region consists of m boundary position

points expressed as (k_{f1}, k_{d1}), (k_{f2}, k_{d2})..., (k_{fm}, k_{dm}) coordinates and their reflections on the true root line. m reflection points can be expressed as (15000, k_{d1}), (15000, k_{d2})..., (15000, k_{dm}) coordinates. In other words, the stability region is surrounded by 2*m points. k_f=15000 can be considered independent of ω because the stability boundary curve is limited to the true root line k_f=15000 (Cem Onat, 2013). As a result, using the coordinate values of the stability boundary curve points and their reflection points, the WGC points of the stability region can be obtained by equations 11 and 12, in Figure 4.

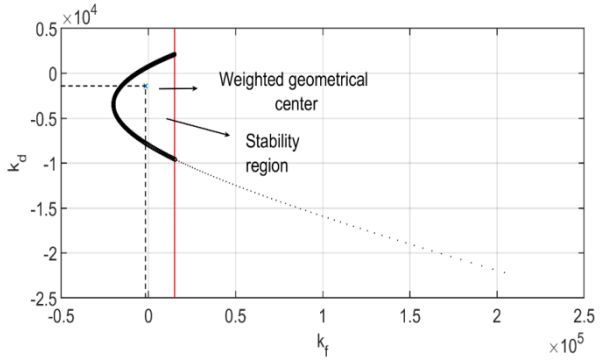

Figure 4. (k_f, k_d) pairs corresponding to each value of ω for stability boundary locus and the weighted geometrical center point.

$$k_{dwgc} = \frac{1}{m}\sum_{i=1}^{m} k_{dj} \quad (11)$$

$$k_{fwgc} = \frac{1}{2m}\left[\sum_{i=1}^{m} k_{fj} + (15000.m)\right] \quad (12)$$

It is a fact that choosing ω with a smaller step size (e.g., 0.05 also results in larger m values) will allow us to get more accurate results than with a larger step size. Results may be affected by step size changes but have no significant effect on stability (Munevver Mine Ozyetkin et al., 2020). Thus, the WGC point of the PD controller is obtained as (k_f, k_d) = (-1703, -1421).

Step 2. The inner loop is reduced using the selected PD control parameters (k_f = -1703, k_d = -1421). Reduced inner loop transfer function is given in equation 13.

$$G(s) = \frac{N(s)}{D(s)} = \frac{G_P(s)}{1+G_{PD}(s)G_P(s)} = \frac{N_P(s)D_{PD}(s)e^{-\tau s}}{D_P(s)D_{PD}(s)+N_{PD}(s)N_P(s)e^{-\tau s}} \quad (13)$$

Step 3. The purpose of the inner loop PD controller is only to achieve stability, but the purpose of the outer loop controller is to both ensure stability and meet the performance requirements of the closed loop system. Accordingly, at this stage of the controller design, the control block diagram is as shown in Figure 5.

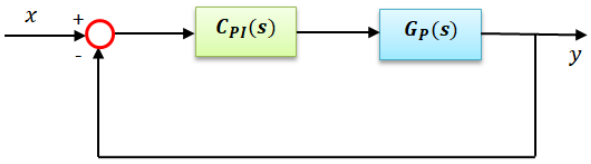

Figure 5. Reduced block diagram.

The stability region is obtained for the PI controller by means of the reduced transfer function in the k_p–k_i plane. PI controller parameters can also be calculated using the given procedure for calculating the C_{PD} parameters. The application of $s = j\omega$ change to the characteristic equation of the outer loop is given in equation 14 (Maslen and Schweitzer, 2009).

$$\Delta_{PI}(j\omega) = D(j\omega)D_{PI}(j\omega) + N(j\omega)N_{PI}(j\omega)e^{-j\tau\omega} = 0 \quad (14)$$

If Δ_{PI} is decomposed into its virtual and real parts (equation 15);

$$\Delta_{PI} = R_{\Delta,PI} + I_{\Delta,PI} = 0 \quad (15)$$

If the procedure described above to obtain the PD controller parameters is also used to obtain the PI parameters, the following equations are obtained. By solving the set of (linear) equations depending on the frequency (ω), the stability region as in Figure 6 and WGC are determined by plotting the obtained k_p and k_i parameters in the k_p – k_i plane in Figure 7. It is a fact that choosing ω with a smaller step size (eg 0.01 also results in larger m values) will allow us to get more accurate results than with a larger step size. Thus, the WGC point of the PI controller is obtained as (k_p, k_i) = (-5185, -20870).

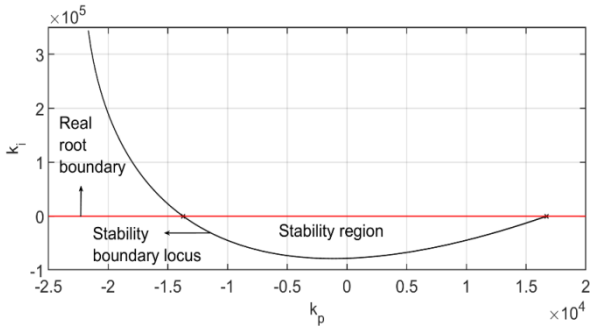

Figure 6. The stability boundary curve and stability region of PD controller

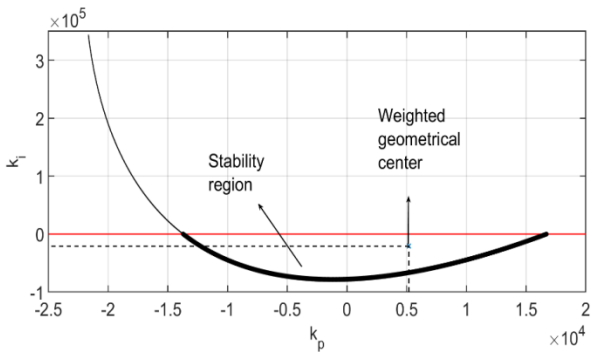

Figure 7. (k_p, k_i) pairs corresponding to each value of ω for stability boundary locus and the weighted geometrical center point.

3. Results and Discussion

Simulations were performed with MATLAB-Simulink software to examine the effectiveness of the proposed control method on the system. In the quarter vehicle

model, the displacement and acceleration responses of the vehicle body were evaluated. In addition, the PSD (Power Spectral Density) response of the system was examined for performance analysis in the frequency domain. ISO 8606 Norm is used for road surface profile classification (Agostinacchio et al., 2014). This standard, in which road pression is classified according to different categories, is often preferred to test control performances in vehicle vibrations (Paksoy & Metin, 2020). An ISO 8608 standard C class road entrance seen in Figure 8 has been applied to the system. Vehicle speed is accepted as 30 m/s.

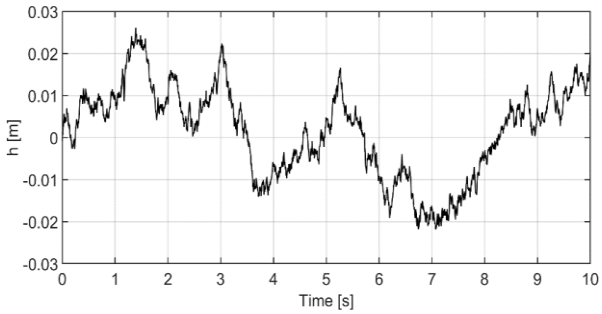

Figure 8. ISO C class road entrance.

In the simulations, the passive situation where there is no control application in the system and the situation with the PI-PD controller designed with the WGC method are compared. The most important data in terms of comfort in vehicles are acceleration responses. Another important data is the displacement responses. Displacement responses are given in Figure 9 and simulation results of acceleration responses are given in Figure 10. It is clearly seen that the controlled state is more effective than the passive state in suppressing both displacement and acceleration responses.

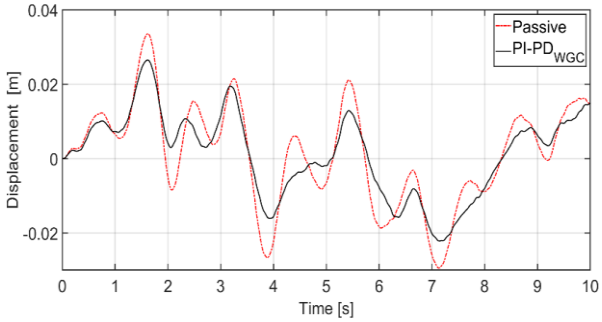

Figure 9. Suspension displacement

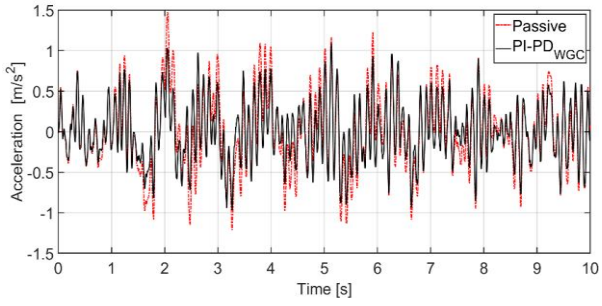

Figure 10. The acceleration of the vehicle body.

In order to analyze the system responses in the frequency domain, the PSD values of the system were examined. Figure 11 shows the acceleration PSD values of the vehicle body. It has been observed that the state in which the controller acts suppress the resonance peaks more effectively than the passive state.

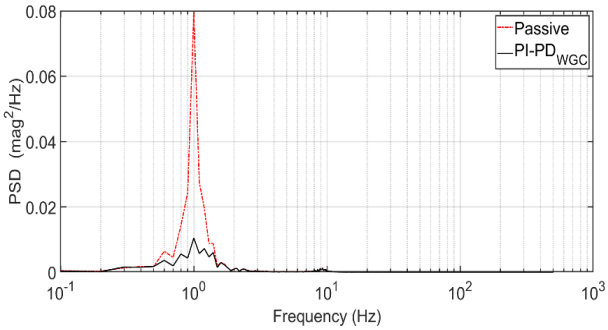

Figure 11. PSD response of vehicle body acceleration.

In order to see the results more clearly, RMS (Root Mean Square) values are given in Table 1 for the numerical evaluation of the system responses. The amount of improvement in displacement RMS value of the body is 16.6%, and in acceleration values it is 21%.

Table 1. RMS values

Control cases	z_1	$\ddot{z}_1$
Passive	0.0141	0.4767
$\mathrm{PI-PD_{WGC}}$	0.0117	0.3765

While evaluating control performance, suspension displacement (z_1-z_2), whose limits are set according to the passive control situation, also needs to be considered. In Figure 12, $\mathrm{PI-PD}_{WGC}$ control condition also reduced suspension displacements.

4. Conclusion

In this study, PI-PD was designed with the WGC method, which is an effective and simple tuning method for a time-delayed quarter vehicle model. The method is based on calculating stabilizing PD and PI controller parameter regions plotted using the stability boundary locus in the (k_f, k_d)-plane and the (k_p, k_i)-plane and computing the weighted geometrical centres of these regions. The proposed method does not use any circular optimization algorithm. The fact that the method allows to calculate the controller parameters numerically on the model offers a good numerical solution to control engineers, especially for practical applications. The simulation results clearly show that the PI PD controller designed with the proposed method for the quarter-car model with the targeted delay time is successful in suppressing the system responses.

Designed using the WGC method, the PI-PD controller can be easily applied to any system class to improve the

performance of processes. In future studies, controller parameters can be optimized with meta-heuristic algorithms using artificial intelligence techniques.

Author Contributions

The percentage of the author contributions is presented below. The author reviewed and approved the final version of the manuscript.

%	A.T.	H.G	M.D.
C	40	30	30
D	50		50
S		100	
DCP	100		50
DAI		50	50
L	50	50	
W	30	40	30
CR	20	20	60
SR			100
PM	20	20	20
FA	20	20	20

C=Concept, D= design, S= supervision, DCP= data collection and/or processing, DAI= data analysis and/or interpretation, L= literature search, W= writing, CR= critical review, SR= submission and revision, PM= project management, FA= funding acquisition.

Conflict of Interest

The authors declared that there is no conflict of interest.

Ethical Consideration

Ethics committee approval was not required for this study because of there was no study on animals or humans.

References

Ahmad I, Shahzad M, Palensky P. 2014. Optimal PID control of magnetic levitation system using genetic algorithm. IEEE International Energy Conference and Exhibition (EnergyCon), May 13-16, Dubrovnik, Croatia, pp: 1-5.

Åström KJ, Hägglund T. 1995. Pid controllers: theory, design, and tuning. The international society of measurement and control. URL: https://aiecp.files.wordpress.com/2012/07/1-0-1-k-j-astrom-pid-controllers-theory-design-and-tuning-2ed.pdf (accessed date: March 21, 2023).

Åström KJ, Hägglund T, Hang CC, Ho WK. 1993. Automatic tuning and adaptation for PID controllers-a survey. Control Eng Pract, 1(4): 699–714.

Atic S, Cokmez E, Peker F, Kaya I. 2018. PID controller design for controlling integrating processes with dead time using generalized stability boundary locus. IFAC, 51: 924–929.

Chidambaram M, Sree RP. 2003. A simple method of tuning PID controllers for integrator/dead-time processes. Comp Chem Engin, 27(2): 211–215.

Ho MT, Datta A, Bhattacharyya SP. 1996. A new approach to feedback stabilization. Proceedings of 35th IEEE Conference on Decision and Control, December 15-17, Kobe, Japan, pp: 4643–4648.

Ho MT, Datta A, Bhattacharyya, SP. 1997. A linear programming characterization of all stabilizing PID controllers. Proceedings of the American Control Conference, June 15-17, New Mexico, Mexico, 6: 3922–3928.

Ho WK, Hang CC, Cao, LS. 1995. Tuning of PID controllers based on gain and phase margin specifications. Automatica, 31(3): 497–502.

Ho WK, Lim KW, Xu W. 1998. Optimal gain and phase margin tuning for PID controllers. Automatica, 34(8): 1009–1014.

Kararsiz G, Paksoy M, Metin M, Basturk, HI. 2021. An adaptive control approach for semi-active suspension systems under unknown road disturbance input using hardware-in-the-loop simulation. Tran Inst Meas Control, 43(5): 995–1008.

Kaya I. 2003. A PI-PD controller design for control of unstable and integrating processes. ISA Trans, 42(1): 111–121.

Kaya I. 2016. PI-PD controllers for controlling stable processes with inverse response and dead time. Electr Eng, 98(1): 55–65.

Kumar EV, Jerome J. 2013. LQR based optimal tuning of PID controller for trajectory tracking of magnetic levitation system. Prodecia Eng, 64: 254–264.

Luyben WL. 2003. Identification and tuning of integrating processes with deadtime and inverse response. Ind Eng Chem Res, 42(13): 3030–3035.

Maslen EH, Schweitzer G. 2009. Magnetic bearings: theory, design, and application to rotating machinery. In Magnetic Bearings. Springer, New York, USA, pp: 521.

Nema S, Padhy PK. 2015. Identification and cuckoo PI-PD controller design for stable and unstable processes. Trans Inst Meas Control, 37(6): 708–720.

Onat C, Daskin M, Turan A, Özgüven ÖF. 2021. Manyetik levitasyon sistemleri için ağırlıklı geometrik merkez yöntemi ile PI-PD kontrolcü tasarımı. Müh Makina, 62: 556–579.

Onat C. 2018. A new design method for PI–PD control of unstable processes with dead time. ISA Trans, 84: 69–81.

Onat C, Sahin M, Yaman Y. 2013. Optimal control of a smart beam by using a luenberger observer. 3rd International Conference of Engineering Against Failure (ICEAF III), 26-28 June, Kos, Greece, pp: 804–811.

Onat C, Turan A, Daskin, M. 2017. WGC based PID tuning method for integrating processes with dead-time and inverse response. International Conference on Mathematics and Engineering, 10 - 12 May, İstanbul, Türkiye, pp: 274-279.

Onat C. 2013. A new concept on PI design for time delay systems: weighted geometrical center. Int Innov Comp Inf Control, 9(4): 1539–1556.

Onat C, Hamamci SE, Obuz S. 2012. A practical PI tuning approach for time delay systems. IFAC Proceed, 45(14): 102–107.

Özbek NS, Eker I. 2016. Gain-scheduled PI-PD based modified Smith predictor for control of air heating system: experimental application. International Mediterranean Science and Engineering Congress, 26-28 October, Adana, Türkiye, pp: 706–715.

Ozyetkin MM, Onat C, Tan N. 2018. PID tuning method for integrating processes having time delay and inverse response. IFAC-PapersOnLine, 51(4): 274–279.

Ozyetkin MM, Onat C, Tan, N. 2019. PI-PD controller design for time delay systems via the weighted geometrical center method. Asian J Control, 22(5): 1811–1826.

Ozyetkin MM, Onat C, Tan, N. 2020. PI-PD controller design for time delay systems via the weighted geometrical center method. Asian J Control, 22(5): 1811–1826.

Padhy PK, Majhi S. 2006. Relay based PI–PD design for stable and unstable FOPDT processes. Comp Chem Eng, 30(5): 790–796.

Pai NS, Chang SC, Huang CT. 2010. Tuning PI/PID controllers for integrating processes with deadtime and inverse response by simple calculations. J Process Control, 6: 726-733.

Paksoy M, Metin M. 2019. Nonlinear semi-active adaptive vibration control of a half vehicle model under unmeasured road input. J Vib Control, 25(18): 2453–2472.

Paksoy M, Metin M. 2020. Nonlinear adaptive semiactive control of a half-vehicle model via hardware in the loop simulation. Turk J Electr Eng Comput Sci, 28(3): 1612–1630.

Park JH, Sung SW, Lee IB. 1998. An enhanced PID control strategy for unstable processes. Automatica, 34(6): 751–756.

Sain D, Swain SK, Mishra SK. 2018. Real Time Implementation of Optimized I-PD Controller for the Magnetic Levitation System using Jaya Algorithm. IFAC-PapersOnLine, 51(1): 106–111.

Tan N. 2009. Computation of stabilizing PI-PD controllers. Int J Control Autom Syst, 7(2): 175–184.

Turan A, Aggumus A. 2021. Implementation of Advanced PID Control Algorithm for SDOF System. J Soft Comp Artif Intell, 2(2): 43–52.

Turan A, Onat C, Şahin M. 2019. Active vibration suppression of a smart beam via PID controller designed through weighted geometric center method. 10th Ankara International Aerospace Conference, AJAC-2019, 13-15 September, Ankara, Türkiye, pp: 79.

Turan A. 2021. Improved optimum PID controller tuning by minimizing settling time and overshoot. in advances in machinery and digitization. URL: https://assets.researchsquare.com/files/rs-844641/v1_covered.pdf?c=1631877580 (accessed date: March 15, 2022).

Yeroglu C, Onat C, Tan N. 2009. A new tuning method for PIλDμ controller. International Conference on Eectrical and Electronics Egineering-ELECO 2009, 5-8 November, Bursa, Türkiye, pp: 12–316.

Zhuang M, Atherton DP. 1993. Automatic tuning of optimum PID controllers. IET Control Theory Appl, 140(3): 216–224.

Ziegler JG, Nichols NB. 1942. Optimum settings for automatic controllers. Transact Amer Soc Mechan Engin, 69(8): 759–765.